Conjugated Polymer-Based Organic Solar Cells

Serap Günes,* Helmut Neugebauer, and Niyazi Serdar Sariciftci

Linz Institute of Organic Solar Cells (LIOS), Physical Chemistry, Johannes Kepler University of Linz, Austria

Contents

1. Introduction

1.1. Prologue

The need to develop inexpensive renewable energy sources stimulates scientific research for efficient, low-cost photovoltaic devices.[1] The organic, polymer-based photovoltaic elements have introduced at least the potential of obtaining cheap and easy methods to produce energy from light.[2] The possibility of chemically manipulating the material properties of polymers (plastics) combined with a variety of easy and cheap processing techniques has made polymer-based materials present in almost every aspect of modern society.[3] Organic semiconductors have several advantages: (a) low-cost synthesis, and (b) easy manufacture of thin film devices by vacuum evaporation/sublimation or solution cast or printing technologies.

Furthermore, organic semiconductor thin films may show high absorption coefficients[4] exceeding 10^5 cm^{-1}, which

* To whom correspondence should be addressed. Telephone: 0090 212 449 1847. Fax: 0090 212 449 1514. E-mail: sgunes@yildiz.edu.tr or serap_gun@yahoo.com. Current address: Yildiz Technical University, Arts and Science Faculty, Physics Department, Davutpasa, Istanbul, Turkey.

makes them good chromophores for optoelectronic applications. The electronic band gap of organic semiconductors can be engineered by chemical synthesis for simple color changing of light emitting diodes (LEDs).[5] Charge carrier mobilities as high as 10 cm^2/V·s[6] made them competitive with amorphous silicon.[7]

This review is organized as follows. In the first part, we will give a general introduction to the materials, production techniques, working principles, critical parameters, and stability of the organic solar cells. In the second part, we will focus on conjugated polymer/fullerene bulk heterojunction solar cells, mainly on polyphenylenevinylene (PPV) derivatives/(1-(3-methoxycarbonyl) propyl-1-phenyl[6,6]C$_{61}$) (PCBM) fullerene derivatives and poly(3-hexylthiophene) (P3HT)/PCBM systems. In the third part, we will discuss the alternative approaches such as polymer/polymer solar cells and organic/inorganic hybrid solar cells. In the fourth part, we will suggest possible routes for further improvements and finish with some conclusions.

The different papers mentioned in the text have been chosen for didactical purposes and cannot reflect the chronology of the research field nor have a claim of completeness. The further interested reader is referred to the vast amount of quality papers published in this field during the past decade.

1.2. Organic Solar Cell Materials

Materials having a delocalized π electron system can absorb sunlight, create photogenerated charge carriers, and transport these charge carriers. Research on organic solar cells generally focuses either on solution processable organic semiconducting molecules/polymers or on vacuum-deposited small-molecular materials.[7]

As an example, phthalocyanine and perylene have commonly found applications in thin film organic solar cells.[1] Phthalocyanine is a p-type, hole conducting material that works as electron donor, whereas perylene and its derivatives show an n-type, electron conducting behavior and serve as electron-acceptor material (see Figure 1).

In general, organic semiconductors can be regarded as "intrinsic wide band gap semiconductors" (band gaps above 1.4 eV) down to "insulators" (band gaps above 3 eV) with a negligibly low intrinsic charge carrier density at room temperature in the dark. Chemical, photochemical, or electrochemical doping is used to introduce extrinsic charge carriers into organic semiconductors.[9] For example, photoinduced electron transfer from a donor to an acceptor-type organic semiconductor film introduces free charge carriers (positive charge carriers on the donor layer, i.e., p-type, and negative charge carriers on the acceptor layer, i.e., n-type). Donor−acceptor-type bilayer devices can thus work like

Serap Günes was born in Istanbul, Turkey, in 1976. She obtained her Ph.D. at the Johannes Kepler University Linz in 2006 under the direction of Professor Niyazi Serdar Sariciftci. She moved to Yildiz Technical University, Istanbul/Turkey, in September 2006 and serves as an Assistant Professor. Besides hybrid solar cells, her research interests include microscopy techniques such as atomic force microscopy (AFM), near field scanning optical microscopy (NSOM), and photovoltaic characterization of organic solar cells and also organic field effect transistors.

Helmut Neugebauer was born in Vienna, Austria, in 1953. He obtained his Ph.D. at the University of Vienna in 1993 under the direction of Professor Neckel. Thereafter, he served as an Assistant Professor at the Institute of Physical Chemistry at the University of Vienna and moved in 1996 to the Johannes Kepler University in Linz, Austria, to the Institute of Physical Chemistry and later to the Linzer Institute of Organic Solar Cells (LIOS). Besides electrochemistry and spectroelectrochemistry of organic semiconductors, his research interests include the photophysical and photovoltaic characterization of organic solar cells. Recently, research subprojects have shifted also toward organic electronics.

Niyazi Serdar Sariciftci is ordinarius professor (chair) and director of the Institute for Physical Chemistry at the Johannes Kepler University in Linz/ Austria. He is the founding director of the Linz Institute of Organic Solar Cells (LIOS) at the same University. He received his Ph.D. in 1989 at the University of Vienna, Austria, in the field of organic semiconducting polymers. After a postdoctoral study period at the physics department of the University of Stuttgart, Germany, he joined in 1992 the Institute for Polymers and Organic Solids at the University of California, Santa Barbara, where he discovered the conjugated polymer-based photovoltaic devices together with Alan Heeger. After moving to Austria in 1996, he pursued the research and technological development of "bulk heterojunction" solar cells at the University of Linz as pioneering work and created related companies.

hexylthiophene) (P3HT), and (iii) derivatives of fluorene backbones such as (poly(9,9′-dioctylfluorene-*co*-bis-*N*,*N*′-(4-butylphenyl-1,4-phenylenediamine) (PFB) (see Figure 1).

1.3. Preparation Techniques

Vacuum evaporation and solution processing techniques are the most commonly used thin film preparation methods in the production of organic solar cells. Polymers decompose under excessive heat and have too large molar mass for evaporation. Therefore, most polymer-based photovoltaic elements are solution processed at low temperatures. The printing/coating techniques are used to deposit conjugated semiconducting polymers.[7] Examples of such techniques used for production of polymer solar cells in the literature are (i) spin-coating, (ii) doctor blading, (iii) screen printing, and (iv) inkjet printing.

Donor−acceptor blends can be prepared by dissolving donor and acceptor components in a common solvent (or solvent mixture). Blends are deposited by using one of the techniques mentioned above. Sometimes, a soluble monomer is cast as a thin film using a postdeposition polymerization reaction afterward. Soluble precursor polymers can also be converted into the final semiconducting form with a post-deposition conversion reaction.[9] The advantage of this latter method is that the resulting conjugated polymer thin films are insoluble.

For organic solar cells, spin-coating, doctor blading, as well as screen-printing methods were applied.[19] Such large-scale printing/coating techniques open up the possibility for an upscaling of the production with low-energy consumption. This is important for the global energy balance, which can be described as the energy delivered by a solar cell during its lifetime as compared to the energy needed to produce the same solar cell itself.

Vacuum evaporation/sublimation is a very clean (no solvent) choice for the deposition of thin films based on small molecules.[7] A vacuum of $<10^{-5}$ mbar is applied to reduce

classical p−n junctions[10,11] (see Figure 2). Chemical doping of a semiconductor matrix by introducing small concentrations of reagents (dopants) has also been reported.[12,15]

The buckminsterfullerene C_{60} is an electron acceptor, which can be electrochemically reduced up to 6 electrons.[16] For photoinduced electron-transfer reactions (i.e., photodoping), it has been blended into electron-donating matrices with hole conducting properties (see Figure 2).[2,17]

The solubility of simple C_{60} is limited. Wudl et al. synthesized a soluble derivative of C_{60}, PCBM (1-(3-methoxycarbonyl) propyl-1-phenyl[6,6]C_{61}),[18] which has been widely used in polymer/fullerene solar cells due to its solubility.

Important representatives of hole conducting donor-type semiconducting polymers on the other side are (i) derivatives of phenylene vinylene backbones such as poly[2-methoxy-5-(3,7-dimethyloctyloxy)]-1,4-phenylenevinylene) (MDMO−PPV), (ii) derivatives of thiophene chains such as poly(3-

Figure 1. Examples of organic semiconductors used in organic solar cells. Reprinted with permission from the Annual Review of Materials and Research, Volume 36, 2006, by Annual Reviews (www.annualreviews.org).
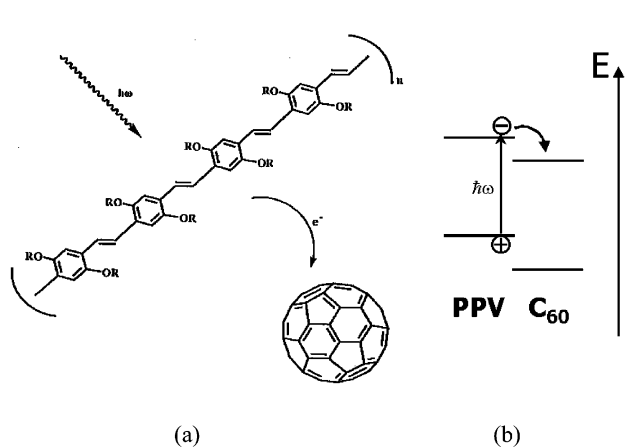
Figure 2. Illustration of the photoinduced charge transfer (a) with a sketch of the energy level (b). After excitation in the PPV polymer, the electron is transferred to the C_{60}.

contaminants like oxygen and water. These can be eliminated further by ultrahigh vacuum (UHV, $<10^{-9}$ mbar) and/or evaporation inside of a glove box with inert atmosphere.[7] To create interpenetrating donor−acceptor networks or to achieve molecular doping, coevaporation techniques are applied.[2,7,20−22]

The general structure used for organic solar cells is similar to the organic light emitting diodes LEDs. The devices are fabricated in sandwich geometry (see Figure 3). As substrates, transparent, conducting electrodes (for example, glass or plastic covered with ITO) are used. ITO (indium tin oxide) electrodes are transparent and conductive but expensive. Alternatives for ITO are searched for, and nanotube network electrodes potentially work as well.[23]

The substrate electrode can be structured by chemical etching. On the transparent conducting substrate, PEDOT: PSS, poly(ethylene-dioxythiophene) doped with polystyrene−sulfonic acid, is coated from an aqueous solution. This PEDOT:PSS layer improves the surface quality of the ITO electrode (reducing the probability of shorts) as well as facilitates the hole injection/extraction. Furthermore, the work function of this electrode can be changed by chemical/electrochemical redox reactions of the PEDOT layer.[24]
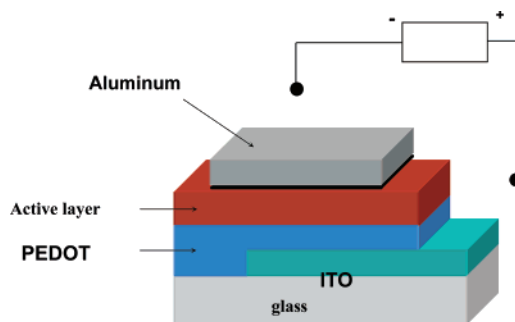
Figure 3. Schematic device structure for polymer/fullerene bulk heterojunction solar cells. The active layer is sandwiched between two contacts: an indium-tin-oxide electrode coated with a hole transport layer PEDOT:PSS and an aluminum top electrode.
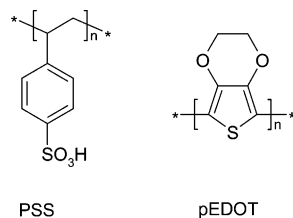
Figure 4. Chemical structure of PEDOT−PSS (poly(3,4-ethylen-dioxythiohene)−polystyrene-*para*-sulfonic acid).

The chemical structures of PEDOT and PSS are shown in Figure 4.

The active layers are coated using solution or vacuum deposition techniques as mentioned above. Finally, the top electrode is evaporated. In general, a lower work-function metal (as compared to ITO) such as aluminum is used with an ultrathin lithium fluoride underlayer. The exact role of this LiF underlayer is unknown, because thicknesses such as ca. 0.6 nm cannot form a closed layer.[25−28] In photoelectron spectroscopy studies, it was shown that the metal work function can be considerably reduced by evaporation of LiF layers.[29]

1.4. Operating Principles

The process of conversion of light into electricity by an organic solar cell can be schematically described by the following steps:[30] absorption of a photon leading to the formation of an excited state, that is, the bound electron−hole pair (exciton) creation; exciton diffusion to a region where exciton dissociation, that is, charge separation occurs; and charge transport within the organic semiconductor to the respective electrodes.[30]

Because of the large band gap in organic materials, only a small portion of the incident solar light is absorbed (see Figure 5). A band gap of 1.1 eV (1100 nm) is capable of absorbing 77% of the solar irradiation on earth.[30] However, the majority of semiconducting polymers have band gaps higher than 2 eV (620 nm), which limits the possible harvesting of solar photons to about 30%.[30] On the other hand, because the absorption coefficients of organic materials are as high as 10^5 cm^{-1}, only 100 nm thickness is enough to absorb most of the photons when a reflective back contact is used.[30] This brings the problem to the point: We need a better "spectral" harvesting of solar photons via lower band gap polymers and/or using energy-transfer cascades. The thicknesses of the films are not the bottleneck.

The primary photoexcitations in organic materials do not directly and quantitatively lead to free charge carriers but to
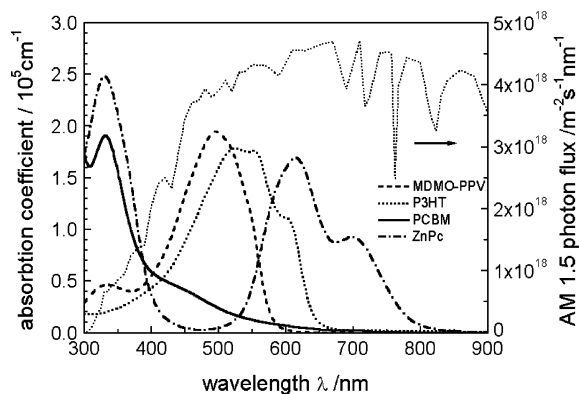
Figure 5. Absorption coefficients of films of commonly used materials are depicted in comparison with the standard AM 1.5 terrestrial solar spectrum.

coulombically bound electron−hole pairs, called excitons. It is estimated that only 10% of the photoexcitations lead to free charge carriers in conjugated polymers.[31] For efficient dissociation of excitons, strong electric fields are necessary. Such local fields can be supplied via externally applied electrical fields as well as via interfaces. At an interface, where abrupt changes of the potential energy occur, strong local electrical fields are possible ($E = -$grad U). Photoinduced charge transfer can occur when the exciton has reached such an interface within its lifetime. Therefore, exciton diffusion length limits the thicknesses of the bilayers.[32] Exciton diffusion length should be at the same order of magnitude as the donor acceptor phase separation length. Otherwise, excitons decay via radiative or nonradiative path ways before reaching the interface, and their energy is lost for the power conversion. Exciton diffusion lengths in polymers and in organic semiconductors are usually around 10−20 nm.[30]

Blending conjugated polymers with electron acceptors, such as fullerenes, is a very efficient way to break apart photoexcited excitons into free charge carriers. Ultrafast photophysical studies showed that the photoinduced charge transfer in such blends happens on a time scale of 45 fs. This is much faster than other competing relaxation processes (photoluminescence usually occurs around 1 ns).[33] Furthermore, the separated charges in such blends are metastable at low temperatures (see Figure 2).

For efficient photovoltaic devices, the created charges need to be transported to the appropriate electrodes within their lifetime. The charge carriers need a driving force to reach the electrodes. A gradient in the chemical potentials of electrons and holes (quasi Fermi levels of the doped phases) is built up in a donor−acceptor junction. This gradient is determined by the difference between the highest occupied molecular (HOMO) level of the donor (quasi Fermi level of the holes) and the lowest unoccupied molecular orbital (LUMO) level of the acceptor (quasi Fermi level of the electrons). This internal electrical field determines the maximum open circuit voltage (V_{oc}) and contributes to a field-induced drift of charge carriers. Also, using asymmetrical contacts (one low work-function metal for the collection of electrons and one high work-function metal for the collection of the holes) is proposed to lead to an external field in short circuit condition within a metal−insulator−metal (MIM) picture.[34] Another driving force can be the concentration gradients of the respective charges, which lead to a diffusion current. The transport of charges is affected

by recombination during the journey to the electrodes, particularly if the same material serves as transport medium for both electrons and holes.[32]

Transport in conjugated polymers is dominated by disorder and was treated in many different studies before. To go into detail to the transport phenomena in conjugated polymers goes beyond the scope of this review, and the interested reader is referred to the different books and articles in the literature and references therein.[32,35−37]

As a last step, charge carriers are extracted from the device through two selective contacts. A transparent indium tin oxide (ITO) matches the HOMO levels of most of the conjugated polymers (hole contact). An evaporated aluminum metal contact with a work function of around 4.3 eV matches the LUMO of acceptor PCBM (electron contact) on the other side.

1.5. Organic Photovoltaic Device Architectures

1.5.1. Bilayer Devices

In a bilayer heterojunction device, p-type and n-type semiconductors are sequentially stacked on top of each other. Such bilayer devices using organic semiconductors were realized for many different material combinations.[1,22,38−44] In such devices, only excitons created within the distance of 10−20 nm from the interface can reach the heterojunction interface. This leads to the loss of absorbed photons further away from the interface and results in low quantum efficiencies.[45] The efficiency of bilayer solar cells is limited by the charge generation 10−20 nm around the donor−acceptor interface (Figure 6). Using thicker films creates optical filter
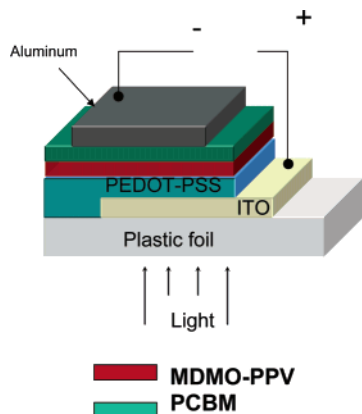
Figure 6. Bilayer configuration in organic solar cells.

effects of the absorbing material before the light gets to the interface, resulting in a minimum photocurrent at the maximum of the optical absorption spectrum.[46] Also, the film thicknesses have to be optimized for the interference effects in the multiple stacked thin film structure.[47,48]

1.5.2. Bulk Heterojunction Devices

Bulk heterojunction is a blend of the donor and acceptor components in a bulk volume (Figure 7). It exhibits a donor−acceptor phase separation in a 10−20 nm length scale. In such a nanoscale interpenetrating network, each interface is within a distance less than the exciton diffusion length from the absorbing site. The bulk heterojunction concept has heavily increased (orders of magnitude) the interfacial area between the donor and acceptor phases and resulted in improved efficiency solar cells.[7]
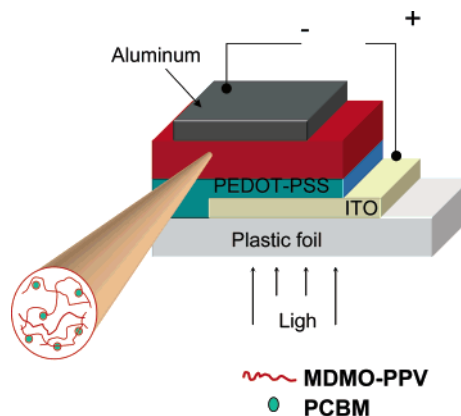
Figure 7. Bulk heterojunction configuration in organic solar cells.

While in the bilayer heterojunction the donor and acceptor phases are completely separated from each other and can selectively contact the anode and cathode, in the bulk heterojunction both phases are intimately intermixed.[7] This mixture has a priori no symmetry breaking in the volume. There is no preferred direction for the internal fields of separated charges; that is, the electrons and holes created within the volume have no net resulting direction they should move.[7] Therefore, a symmetry breaking condition (like using different work-function electrodes) is essential in bulk heterojunctions. Otherwise, only concentration gradient (diffusion) can act as driving force. Furthermore, separated charges require percolated pathways for the hole and electron transporting phases to the contacts. In other words, the donor and acceptor phases have to form a nanoscale, bicontinuous, and interpenetrating network.[49] Therefore, the bulk heterojunction devices are much more sensitive to the nanoscale morphology in the blend, which will be discussed in more detail below.

Bulk heterojunctions can be achieved by co-deposition of donor and acceptor pigments[14,20,21,50] or solution casting of either polymer/polymer,[44,51,52] polymer/molecule,[22,54,57] or molecule/molecule[58,59] donor−acceptor blends.[55,60]

1.6. Characterization of a Solar Cell Device

The current−voltage characteristics of a solar cell in the dark and under illumination are shown in Figure 8. In the dark, there is almost no current flowing, until the contacts start to inject at forward bias for voltages larger than the open circuit voltage. In the fourth quandrant (between (a) and (b)), the device generates power under light. At maximum power point (MPP), the product of current and voltage is the largest.[7]

The photovoltaic power conversion efficiency of a solar cell is determined by the following formula:

$$\eta_e = \frac{V_{oc} * I_{sc} * FF}{P_{in}}$$

$$FF = \frac{I_{mpp} * V_{mpp}}{I_{sc} * V_{oc}}$$

where V_{oc} is the open circuit voltage, I_{sc} is the short circuit current, FF is the fill factor, and P_{in} is the incident light power density. This light intensity is standardized at 1000 W/m^2 with a spectral intensity distribution matching that of the sun on the earth's surface at an incident angle of 48.2°,
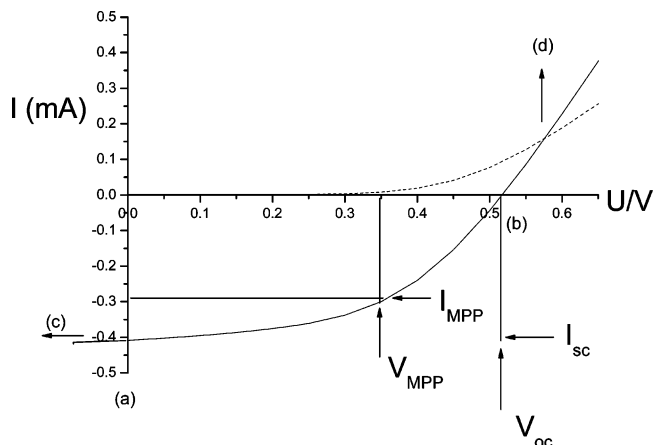
Figure 8. Current−voltage (I−V) curves of an organic solar cell (dark, - - -; illuminated, −). The characteristic intersections with the abscissa and ordinate are the open circuit voltage (V_{oc}) and the short circuit current (I_{sc}), respectively. The largest power output (P_{max}) is determined by the point where the product of voltage and current is maximized. Division of P_{max} by the product of I_{sc} and V_{oc} yields the fill factor *FF*.

which is called the AM 1.5 spectrum.[61] I_{mpp} and V_{mpp} are the current and voltage at the maximum power point.

1.6.1. Critical Parameters for Solar Cell Efficiency

Open Circuit Voltage. Generally, the open circuit voltage of a metal−insulator−metal (MIM) device is determined by the difference in work functions of the two metal contacts.[34] However, in a p−n junction, the maximum available voltage is determined by the difference of the quasi Fermi levels of the two charge carriers, that is, n-doped semiconductor energy level and p-doped semiconductor energy level, respectively. In organic solar cells, the open circuit voltage is found to be linearly dependent on the highest occupied molecular orbital HOMO level of the donor (p-type semiconductor quasi Fermi level) and lowest unoccupied molecular orbital LUMO level of the acceptor (n-type semiconductor quasi Fermi level).[62,63]

Brabec et al. clearly showed linear correlation of the first reduction potential (LUMO level) of the fullerene acceptors (different derivatives of fullerene C_{60} in that study) and the observed open circuit potential (see Figure 9).[62]
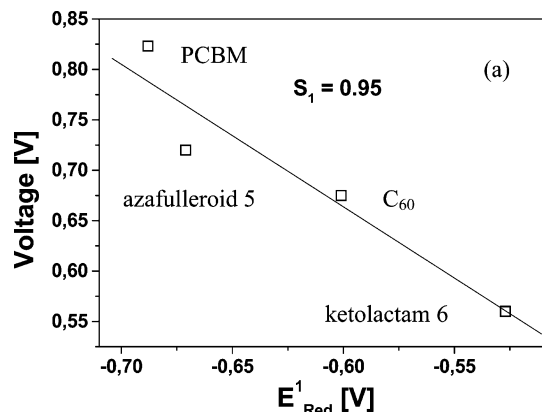
Figure 9. V_{oc} of different bulk heterojunction solar cells plotted versus the reduction potential/LUMO position of the acceptor fullerene derivative used in each individual device. Reused with permission from C. J. Brabec, A. Cravino, D. Meissner, N. S. Sariciftci, T. Fromherz, M. Minse, L. Sanchez, and J. C. Hummelen, *Advanced Functional Materials, 11*, 374 (2001). Copyright 2001, Wiley-VCH Verlag GmbH, D69469 Weinheim.

Gadisa et al.[64] studied the changes in the V_{oc} with the variation of the first oxidation potential (HOMO level) of the donor conjugated polymer. Scharber et al.[63] reported for 26 different bulk heterojunction solar cells that there is a linear relation between the oxidation potential (HOMO level) of the conjugated polymer and the V_{oc} (see Figure 10).
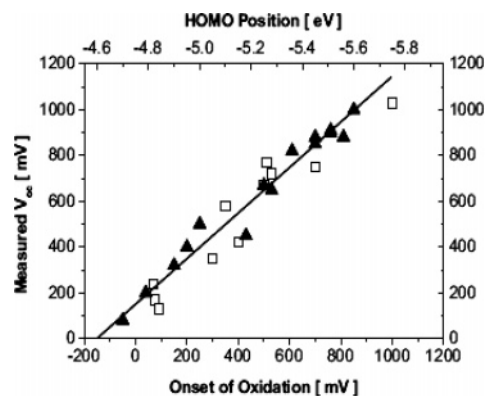
Figure 10. V_{oc} of different bulk heterojunction solar cells plotted versus the oxidation potential/HOMO position of the donor polymer used in each individual device. The straight line represents a linear fit with a slope of 1. Reused with permission from M. Scharber, D. Mühlbacher, M. Koppe, P. Denk, C. Waldauf, A. J. Heeger, and C. Brabec, *Advanced Materials, 18*, 789 (2006). Copyright 2006, Wiley-VCH Verlag GmbH&Co. KGaA, Weinheim.

Charge carrier losses at electrodes lower the V_{oc}.[64] Open circuit voltage is also affected by the nanomorphology of the active layer in the polymer fullerene bulk heterojunction solar cells.[65]

To achieve a better match between the energy levels of the anode and the HOMO of the hole conducting material, the commonly used indium tin oxide (ITO) anode can be modified by plasma etching[66,67] or by coating with a higher work function organic hole transport layer.[68,69] Ganzorig et al. demonstrated that self-assembled monolayers (SAM) of polar molecules can modify the work function of ITO by up to 0.9 eV.[70]

The cathode is generally modified by deposition of a thin layer of LiF between the metal electrode and the organic semiconductor. This improves the charge injection in organic light emitting diodes OLEDs[26,27] and also increases V_{oc} in organic solar cells.[25]

Interfacial effects at the metal/organic semiconductor interface (such as oxide formation) change the work function of the electrodes and influence the open circuit potential.[71,72]

In conclusion, the open circuit potential is a sensitive function of energy levels of the used materials as well as their interfaces.[7]

Short Circuit Current. In the ideal, loss free contacts, the short circuit current, I_{sc}, is determined by the product of the photoinduced charge carrier density and the charge carrier mobility within the organic semiconductors:

$$I_{sc} = ne\mu E$$

where n is the density of charge carriers, e is the elementary charge, μ is the mobility, and E is the electric field.

Assuming the 100% efficiency for the photoinduced charge generation in a bulk heterojunction mixture, n is the number of absorbed photons per unit volume.

For a given absorption profile of a given material, the bottleneck is the mobility of charge carriers. Mobility is not

a material parameter but a device parameter. It is sensitive to the nanoscale morphology of the organic semiconductor thin film.[73−77] In a van der Waals crystal, the final nano-morphology depends on film preparation. Parameters such as solvent type, the solvent evaporation (crystallization) time, the temperature of the substrate, and/or the deposition method can change the nanomorphology.[78,79] The formation of a bulk heterojunction enhances the interfacial area between donor and acceptor phases; however, the prize paid is the compli-cated nanomorphology of a blend that is difficult to optimize and control.[73]

The external quantum efficiency or incident photon to current efficiency (IPCE) is simply the number of electrons collected under short circuit conditions, divided by the number of incident photons. IPCE is calculated using the following formula:

$$\text{IPCE} = \frac{1240 I_{sc}}{\lambda P_{in}}$$

where λ [nm] is the incident photon wavelength, I_{sc} [$\mu A/cm^2$] is the photocurrent of the device, and P_{in} [W/m^2] is the incident power.

Fill Factor. Fill factor is determined by charge carriers reaching the electrodes, when the built-in field is lowered toward the open circuit voltage. In fact, there is a competition between charge carrier recombination and transport. Hence, the product of the lifetime τ times the mobility μ determines the distance d that charge carriers can drift under a certain electric field E: $d = \mu*\tau*E$. This product $\mu*\tau$ has to be maximized.[80] Furthermore, the series resistances influence the filling factor considerably and should be minimized. Finite conductivity of the ITO substrate clearly limits the *FF* on large area solar cells.[12] Finally, the device should be free of "shorts" between electrodes to maximize the parallel shunt resistance.

1.7. Stability

Apart from the necessity for efficiency improvement, stability is another problem for organic solar cells. Especially under light illumination and by simultaneous exposure to oxygen or water vapor, a rapid photooxidation/degradation occurs. Protection from air and humidity is necessary to achieve long device lifetimes.[81]

Neugebauer et al.[82] showed that the photodegradation of the conjugated polymer is significantly decreased when mixed with fullerenes. The stability of the conjugated polymer−fullerene solar cell mixture, which forms a charge-transfer donor and acceptor couple, is higher than the stability of conjugated polymers in light emitting diodes.[83] Also, *I−V* curves confirmed better stability of solar cell mixtures as compared to LEDs with a single polymeric component. The stabilization effect of C_{60} is presumed to be due to the fast electron transfer. In this process, the highly reactive excited state of the polymer is emptied rapidly, lowering the energy to the more environmentally stable electrochemical potentials of fullerene reduction (LUMO).

MDMO−PPV/PCBM solar cells show also a significant nanomorphological degradation.[84] At elevated temperatures, the PCBM molecules can diffuse through the MDMO−PPV matrix and form large crystals.[74,75,85] This nanomorphological instability can be fixed by post production cross-linking of the components, to prevent their diffusion.[86]

Poly(3-heyxlthiophene)/PCBM blends show much better photostability. The efficiency of solar cells using these components changed less than 20% during 1000 h of light soaking at 70 °C under an inert atmosphere.[87]

2. Conjugated Polymer: Fullerene-Based Solar Cells

Photoinduced electron transfer from donor-type semicon-ducting polymers onto acceptor-type polymers or molecules, such as C_{60},[30] is utilized in these organic solar cells. Bilayers of semiconducting polymers with fullerenes show low photovoltaic conversion efficiency.[43] Significant improve-ment has been achieved by using phase-separated composite materials. Controlling the nanomorphology of the phase separation in an interpenetrating network ("bulk heterojunc-tion")[54] has increased the power conversion efficiency of solar cells made from MDMO−PPV/C_{60} significantly.[88,89] Typical dimensions of phase separation have to be within the exciton diffusion length (on the order of 10 nm). On the other hand, bicontinuous, undisturbed pathways have to be ensured for transport of charge carriers to the electrodes.[87]

To enhance charge carrier transport in organic and polymeric materials, we have to increase the mesoscopic order and crystallinity. Hence, a nanoscale interpenetrating network with crystalline order of both constituents seems a desirable architecture for the active layer of polymer pho-tovoltaic devices.[59,87] Eventually, the electronic band gaps of the materials in the photoactive layer should be tuned to harvest more light from the solar spectrum.[87]

2.1. PPV:PCBM Bulk Heterojunction Solar Cells

2.5% efficient solar cells can be obtained from soluble derivatives of phenylene-vinylenes, for example, poly[2-methoxy-5-(3′,7′-dimethyloctyloxy)-1,4-phenylene vinylene) (MDMO−PPV) mixed with soluble derivatives of fullerenes, for example, 1-(3-methoxycarbonyl)propyl-1-phenyl-[6,6]-methanofullerene (PCBM).[88] Shaheen et al. showed that a power conversion efficiency of 2.5% under AM 1.5 condi-tions can be obtained by using chlorobenzene as a solvent for spincasting in the weight ratio of 1:4 for MDMO−PPV: PCBM.[88] Changing the solvent from toluene to chloroben-zene increases the efficiency by nearly a factor of 3, which was assigned to originate from the changes in the nanomor-phology (see Figure 11).[88]

Such bulk heterojunction solar cells have 80 wt % PCBM.[88] However, the polymer MDMO−PPV is supposed to be the main light absorber in these solar cells, because PCBM has almost no absorption in the visible-near-infrared region. Therefore, it is better to increase the volume concentration of MDMO−PPV for better absorption of solar light.[73]

The electron mobility of pure PCBM[90] was reported to be higher ($\sim 10^{-3}$ cm²/V·s) than the hole mobility of pure MDMO−PPV (10^{-4} cm²/V·s). The interesting observation is also that the mobility of the holes in the mixture is increasing with increasing fullerene loading. This is coun-terintuitive because the admixture of fullerene should have introduced more defects and lowered the hole mobility.[92−98]

To study the relation between morphology and perfor-mance in bulk heterojunction solar cells, MDMO−PPV/ PCBM blends were investigated in detail.[73,75−77,85] Experi-mentally, the following parameters have been identified as influencing the nanoscale morphology in these polymer−
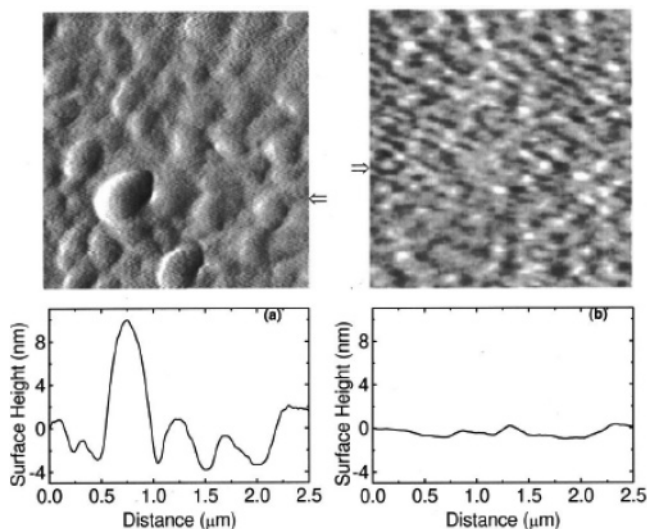
Figure 11. AFM images showing the surface morphology of MDMO−PPV:PCBM (1:4 by wt) blend films spin-coated from (a) toluene and (b) chlorobenzene solutions. The films cast from chlorobenzene have a smoother surface as compared to films cast from toluene. Reused with permission from Sean Shaheen, Christoph J. Brabec, N. Serdar Sariciftci, Franz Padinger, Thomas Fromherz, and Jan C. Hummelen, *Applied Physics Letters*, *78*, 841 (2001). Copyright 2001, American Institute of Physics.

fullerene blends: (i) the used solvent, (ii) processing temperature, (iii) the relative ratio in composition between polymer and fullerene, (iv) the solution concentration, (v) thermal annealing, and (vi) the primary chemical structure of the materials determining tertiary organization structures.

The primary chemical structures of polymer and fullerene determine the solubility in organic solvents and the miscibility between these two compounds. The solvent itself furthermore influences the drying time during film formation, whereas thermal annealing enables the recrystallization. Diffusion of one or both components in the blend leads to a modification of the phase separation.[7]

The combination of atomic force microscopy (AFM), scanning electron microscopy (SEM), and transmission electron microscopy (TEM) was applied to compare the nanomorphology of chlorobenzene and toluene cast blends.[73−75]

Martens et al. showed by TEM[77] that larger (>50 nm) PCBM-rich domains are embedded in a matrix of a saturated mixture of MDMO−PPV and PCBM.[75] Hoppe et al.[75] demonstrated that increasing PCBM content increases the size of these PCBM nanoclusters (see Figure 12).

Cross-sectional SEM images show (Figure 13) that these PCBM nanoclusters are covered by another "skin" layer of approximately 20−40 nm thickness. 10−15 nm-sized nanospheres are found in the composites and assigned to pure polymer coils. These nanoclusters are embedded in an amorphous matrix of saturated solid-state solution of both phases in each other.[75]

Van Duren et al.[73] investigated the phase separation and performance of solar cells based on MDMO−PPV as a donor and PCBM as an acceptor. Using AFM, TEM, dynamic time-of-flight secondary ion mass spectrometry (TOF-SIMS), and time-correlated single photon counting, they demonstrated the nanoscale phase separation at approximately 67 wt % PCBM giving rise to almost pure PCBM domains in a surrounding matrix of MDMO−PPV that contains up to 50 wt % PCBM.
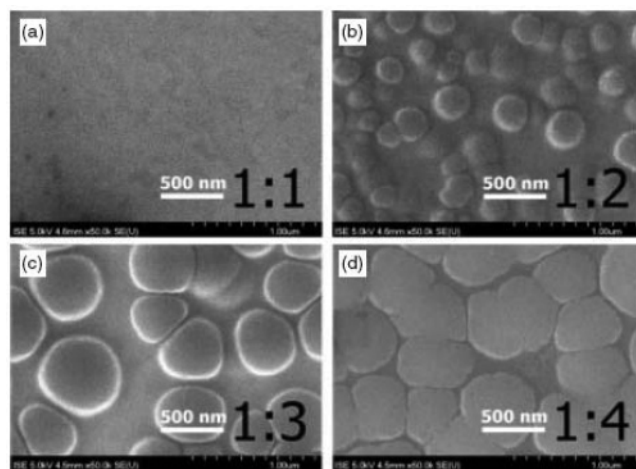
Figure 12. Top views of films cast from toluene with various weight ratios of MDMO−PPV to PCBM using SEM. Reused with permission from H. Hoppe, M. Niggemann, C. Winder, J. Kraut, R. Hiesgh, A. Hinsch, D. Meissner, and N. S. Sariciftci, *Advanced Functional Materials*, *14*, 1005 (2004). Copyright 2004, Wiley-VCH Verlag GmbH&Co. KGaA, Weinheim.
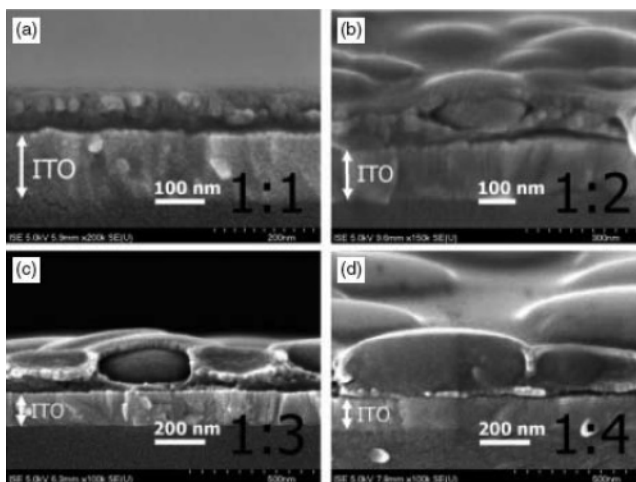
Figure 13. SEM cross sections of MDMO−PPV/PCBM blend film cast from toluene with various weight ratios of MDMO−PPV and PCBM. Reused with permission from H. Hoppe, M. Niggemann, C. Winder, J. Kraut, R. Hiesgh, A. Hinsch, D. Meissner, and N. S. Sariciftci, *Advanced Functional Materials*, *14*, 1005 (2004). Copyright 2004, Wiley-VCH Verlag GmbH&Co. KGaA, Weinheim.

Replacing the C_{60} moiety of [60]PCBM by C_{70} fullerene derivative makes the HOMO−LUMO transitions slightly more allowed and increases the light absorption/harvesting[99,100] (see Figure 14).

Wienk et al.[100] demonstrated improved efficiency for bulk heterojunction solar cells in an isomeric mixture of C_{70} derivatives mixed with MDMO−PPV. Solar cells of this kind are best when prepared from *ortho*-dichlorobenzene (ODCB) solution, giving power conversion efficiency $\eta = 3\%$ under AM 1.5 (see Figure 15).

2.2. Poly(3-alkylthiophene):PCBM Bulk Heterojunction Solar Cells

Poly(3-alkylthiophenes) (P3ATs) are conjugated polymers with good solubility, processability, and environmental stability.[101,102] Regioregular poly(3-alkylthiophenes) (RR-P3AT) (P3HT:poly(3-hexylthiophene), P3OT:poly(3-octylthiophene), and P3DDT:poly(3-dodecylthiophene) are used
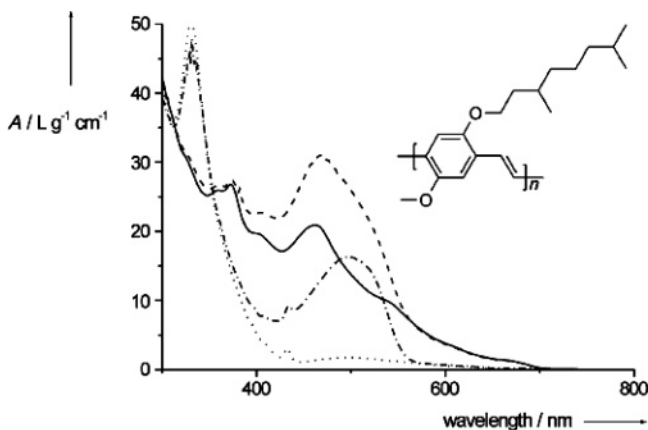
Figure 14. UV/vis spectra of [70]PCBM (−) and [60]PCBM (···) both in toluene. To illustrate the contribution of MDMO−PPV to the absorption, the (normalized) spectra of [70]PCBM: MDMOPPV (4:1, w/w; − − −) and [60]PCBM:MDMO−PPV (4:1, w/w; − · − · −), also in toluene, are also presented. The inset shows the structure of MDMO−PPV. Reused with permission from M. Wienk, J. M. Kroon, W. J. H. Verhees, J. Krol, J. C. Hummelen, P. Van Haal, and R. A. J. Janssen, *Angewandte Chemie, International Edition*, *42*, 3371 (2003). Copyright 2003, Wiley-VCH Verlag GmbH&Co. KGaA, Weinheim.

as electron donors in polymer:fullerene bulk heterojunction solar cells with record power conversion efficiencies up to 5%.[103]

Al Ibrahim et al.[104] investigated the influence of the alkyl side chain length of regioregular P3HT, P3OT, and P3DDT on the electrochemical and optical properties. Energy levels for P3OT,[105] for P3HT,[106,107] and for P3DDT[107] were almost the same with the optical band gap energy around 1.9 eV. With longer side chain length, their electrochemical band gaps were slightly increased. The absorption coefficient undergoes a systematic decrease by longer side chain polythiophenes due to chromophore dilution (i.e., conjugated segments in ratio to nonconjugated segments decrease upon increasing the side chain length).

Using regioregular poly(3-hexylthiophene) (RR-P3HT) as donor and PCBM as acceptor,[60,108] bulk heterojunction solar cells have been realized with external quantum efficiencies of around 75% and power conversion efficiencies up to 5%.[109] The high efficiency of these devices is proposed to be due to a microcrystalline lamellar stacking in the solid-state packing.[110] Resulting in reduced recombination,[84] RR-P3HT gives a hole mobility up to ∼0.1 cm²/V·s.[111,112] Moreover, interchain interactions cause a red shift of the optical absorption of RR-P3HT due to this stacking. The second component, PCBM, has an electron mobility of 2 × 10⁻³ cm²/V·s.[113]

The efficiency of solar cells based on P3HT has been improved by a thermal annealing step.[60,102,114] Padinger et al. demonstrated that, by annealing the devices by simultaneously applying an external voltage, the characteristics of such plastic solar cells are improved[60] (see Figure 16). Annealing not only causes recrystallization but also reduces the free volume and the density of defects at the interfaces.[115] P3HT recrystallization has a positive effect on the mobility of holes.[116] Thermal annealing under chloroform vapor[117] or simple thermal treatment[114] leads to an overall increase in power conversion efficiency.

Chiravaze[102] et al. showed that the optical absorption spectrum shows a pronounced red shift upon thermal annealing. Al Ibrahim et al. reported on the effects of the
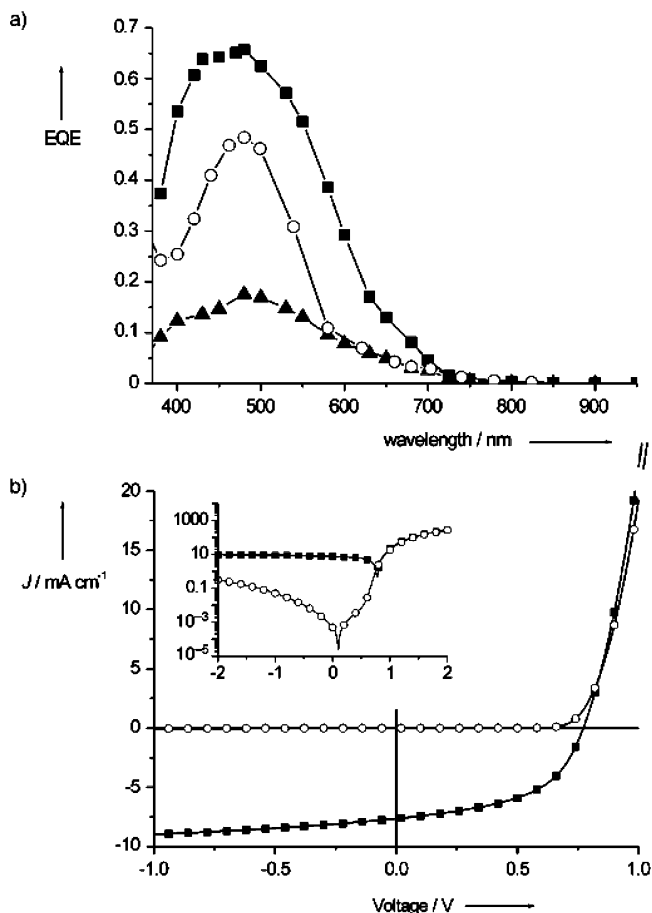
Figure 15. Photovoltaic properties of an ITO/PEDOT−PSS/ fullerene:MDMO−PPV/LiF/Al device with an active area of 0.1 cm². (a) External quantum efficiency (EQE) of [70]PCBM: MDMO−PPV cells spin-coated from chlorobenzene (▲) and ODCB (■) and of [60]PCBM:MDMO−PPV devices spin-coated from chlorobenzene (○); (b) current−voltage characteristics of [70]-PCBM:MDMO−PPV cells spin-coated from ODCB, in the dark (○) and under illumination (AM 1.5, 1000 W/m²; ■). The inset shows the dark and illuminated *I/V* curves in a semilogarithmic plot. Reused with permission from M. Wienk, J. M. Kroon, W. J. H. Verhees, J. Krol, J. C. Hummelen, P. Van Haal, and R. A. J. Janssen, *Angewandte Chemie International Edition*, *42*, 3371 (2003). Copyright 2003, Wiley-VCH Verlag GmbH&Co. KGaA, Weinheim.

processing conditions on the light absorption of P3HT:PCBM cells (Figure 17).[118] Films cast from chloroform and chlorobenzene solutions have absorption maxima at 600 and 630 nm, respectively.[119] The authors argued that these differences indicated a higher degree of P3HT side chain ordering[120] using chlorobenzene. The increased structural order can be created by thermal annealing and/or by changing the solvent from chloroform to chlorobenzene.[119]

The correlation between the structural and optical properties was reported by Erb et al. using the grazing incidence X-ray diffraction (XRD, Figure 18).[121] A higher crystallinity of the P3HT:PCBM films is observed upon annealing.[121]

Savenije et al.[123] studied the relationship between the morphology and charge carrier mobility using the flash photolysis time-resolved microwave conductivity technique (FP-TRMC). Annealing at 80 °C resulted in the formation of crystalline P3HT fibrils and enhanced the hole mobility by an order of magnitude.

For a comprehensive analysis of the transport in polymer fullerene solar cells, the reader is referred to extended
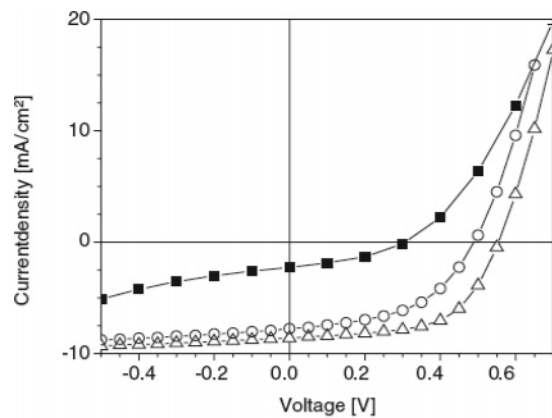
(a)
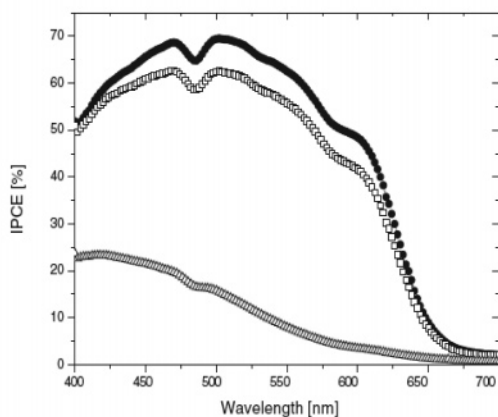
(b)

Figure 16. (a) Current−voltage characteristics of P3HT−PCBM solar cells under illumination: as-produced solar cells (■), annealed solar cell (○), and cell simultaneously treated by annealing and applying external electric field (△). (b) Incident photon to current efficiency (IPCE) of P3HT−PCBM solar cells: as-produced solar cell (△), annealed solar cell (□), and cell simultaneously treated by annealing and applying an external voltage (●). Reused with permission from F. Padinger, R. Rittberger, and N. S. Sariciftci, *Advanced Functional Materials*, *13*, 85 (2003). Copyright 2003, Wiley-VCH Verlag GmbH&Co. KGaA, Weinheim.

literature on this topic.[91−96] Briefly mentioning, the charge carrier mobility in bulk heterojunction solar cells was studied using field effect transistors (FET),[124,125] time-of-flight (TOF),[126] and space charge limited current (SCLC) in a sandwich structure.[127] Usually, the electron and the hole mobility in organic solar cells are unbalanced. The mobility of holes in MDMO−PPV thin films is several orders of magnitude lower than the electron mobility in PCBM thin films.[127] Charge carrier mobility and recombination in bulk heterojunction solar cells was studied using a novel method: the charge extraction by a linear increase of voltage (CELIV). In the CELIV technique, the equilibrium charge carriers are extracted from a dielectric under a reverse bias voltage ramp. The CELIV technique can be used to determine charge carrier mobilities in samples with only a few hundred nanometer thickness.[91]

Mihailetchi et al.[98] developed a model for quantitative description of the behavior of PPV:PCBM bulk heterojunction solar cells. Injection currents that quadratically scale with the voltage are indicative of space charge limited transport. This observation is common for low mobility, disordered semiconductors, and it allows for a direct determination of
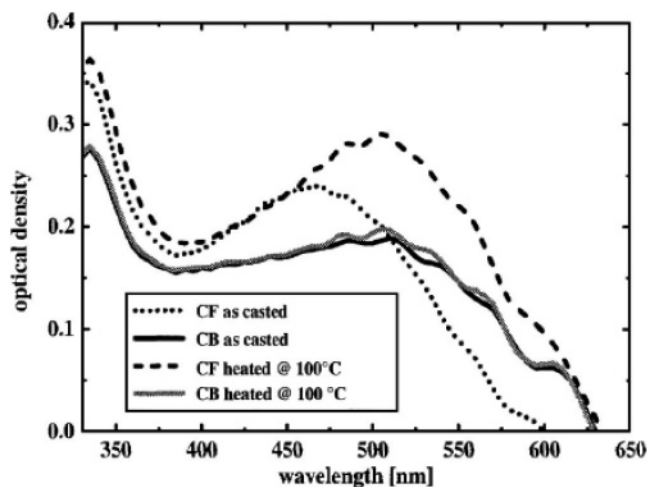
Figure 17. Absorption spectra of P3HT:PCBM composite films (1:2 wt %) cast from chloroform and chlorobenzene solutions before and after thermal heating at 100 °C. Reused with permission from M. Al Ibrahim, O. Ambacher, S. Sensfuss, and G. Gobsch, *Applied Physics Letters*, *86*, 201120 (2005). Copyright 2005, American Institute of Physics.
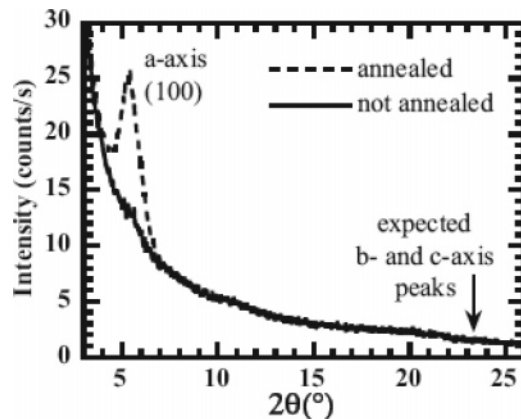
Figure 18. Diffractogram (grazing incidence) of P3HT/PCBM composite films deposited on glass/ITO/PEDOT−PSS. Reused with permission from T. Erb, U. Zhokhavets, G. Gobsch, S. Raleva, B. Stühn, P. Schilinsky, C. Waldauf, and C. J. Brabec, *Advanced Functional Materials*, *15*, 1193 (2005). Copyright 2005, Wiley-VCH Verlag GmbH&Co. KGaA, Weinheim.

the SCLC mobility.[128−132] By simply annealing the devices at a temperature above 110 °C for 4 min, hole mobility in the P3HT (Figure 19) phase increased by more than 3 orders of magnitude.[98]

Using the CELIV method by Mozer et al.[91] reported a negative electric field dependence of mobility in P3HT.

In thin film organic photovoltaic cells, the bulk heterojunction layer is sandwiched between two charge selective electrodes (Figure 20). The electric field of the light has to become zero at the metallic (Al) back electrode due to reflection condition for a standing wave. Thus, a fraction of the active layer has nearly vanishing electrical field of light.[133]

Kim et al.[109] [Heeger 5%] introduced an optically transparent spacer between the active layer and the Al electrode. The spacer must be a good electron transport material with a conduction band edge equal to or lower in energy than that of the LUMO of the PCBM, and it must be transparent to light. Such a spacer is intended to push the optically absorbing region away from the reflecting metal electrode. Titanium dioxide was used as spacer and under AM 1.5
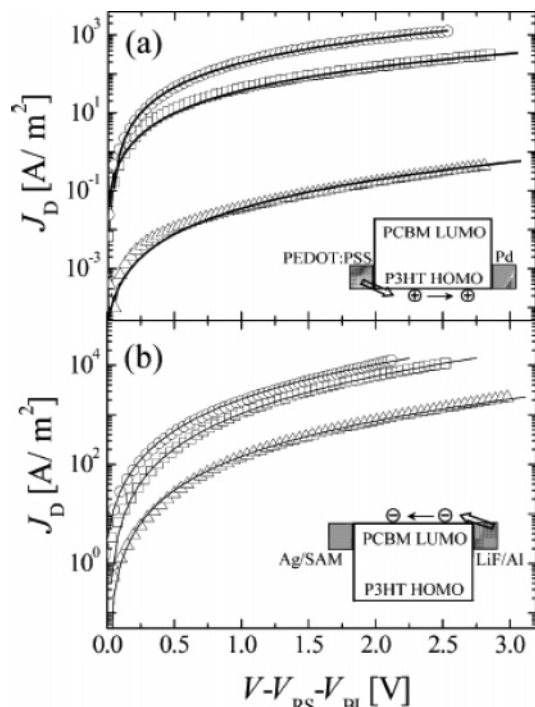
Figure 19. Dark current densities of 50:50 wt % P3HT:PCBM blend devices measured at room temperature in the hole only (a) and electron only (b) device configurations. The symbols correspond to different annealing temperatures of the photoactive layer as follows: as-cast (Δ), 90 °C (□), and 120 °C (○), respectively. Reused with permission from V. Mihailetchi, K. K. Van Duren, P. Blom, J. C. Hummelen, R. Janssen, J. Kroon, M. Rispens, W. Verhees, and M. Wienk, *Advanced Functional Materials*, *16*, 699 (2006). Copyright 2006, Wiley-VCH Verlag GmbH&Co. KGaA, Weinheim.
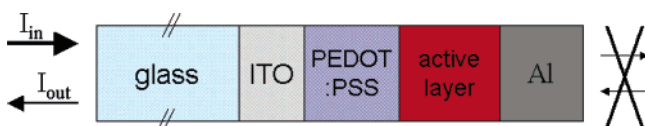
Figure 20. Schematic structure of the modeled multilayer device. The incoming light (I_{in}) enters the device and propagates attenuated toward the aluminum electrode. There it is reflected, and the outgoing intensity (I_{out}) leaves the device through the glass. Because of the high reflectivity of the sufficiently thick aluminum electrode, no light leaves or enters from the right side of the device. Reprinted from *Thin Solid Films*, *451−452*, H. Hoppe and N. S. Sariciftci, p 587, Copyright 2004, with permission from Elsevier.

illumination of 90 mW/cm^2 devices showed $I_{sc} = 11.1$ mA/cm^2, $V_{oc} = 0.61$ V, and $FF = 0.66$, corresponding to improved power conversion efficiency of around 5% (Figure 21).[109]

3. Alternative Approaches

3.1. Polymer/Polymer Solar Cells

Inspired by the developments of conjugated polymer/ fullerene bulk heterojunctions, similar systems are also reported in the literature. Polymer/polymer bulk heterojunction solar cells achieved considerably less efficiencies and attracted less attention, although they might have the potential to be implemented in inexpensive, large area photovoltaic systems, as well.

Bulk heterojunctions of two conjugated polymers[44,51] have several advantages. In a conjugated polymer blend, both
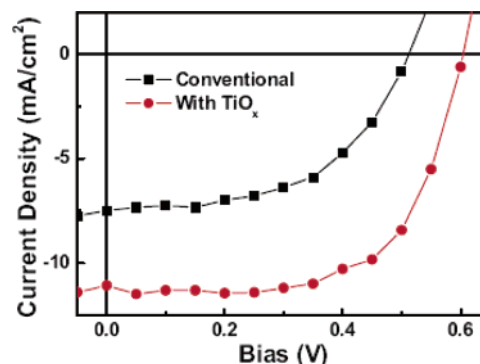
Figure 21. The current density−voltage characteristics of polymer solar cells with (●) and without (■) the TiO$_x$ optical spacer. Reused with permission from J. Kim, S. Kim, H. Lee, K. Lee, W. Ma, X. Huong, and A. J. Heeger, *Advanced Materials, 18*, 572 (2006). Copyright 2006, Wiley-VCH Verlag GmbH&Co. KGaA, Weinheim.

components can exhibit a high optical absorption coefficient and cover complementary parts of the solar spectrum. It is relatively easy to tune both components individually to optimize optical properties, charge transfer, and charge collection processes. On the other hand, polymer blends have an intrinsic tendency to phase separate. These phase-separated domains usually have dimensions of several micrometers and are thus too large as compared to exciton diffusion length limitations for polymeric cells (see discussion in section 1.5). The biggest challenge for the polymer/polymer bulk heterojunction concept is to identify suitable n-type polymers with acceptor properties and good stability.[134]

3.2. Donor−Acceptor "Double Cable" Polymers

The concept of "double cable" polymers has been introduced to have a control on the morphology at the molecular level (see Figure 22).[135] Chemically attaching the electron
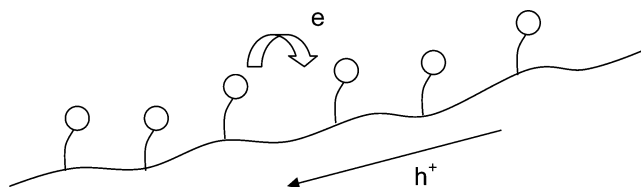
Figure 22. Schematic representation of "double cable" polymers. The charge carriers generated by photoinduced charge transfer can be in principle transported within one molecule, therefore termed as a "molecular heterojunction".

acceptor moieties directly to the donor polymer backbone prevents the phase separation.

Electrons created by photoinduced electron transfer are transported by hopping between the pendent acceptor moieties, leaving the remaining hole on the conjugated chain transporting the positive charge. Several double cable materials have been explored in polymer solar cells. The efficiency of such devices is low probably due to fast recombination or inefficient interchain transport.[136]

3.3. Hybrid Solar Cells

A hybrid solar cell consists of a combination of both organic and inorganic semiconducting materials. It combines the unique properties of inorganic semiconductors with the film-forming properties of the conjugated polymers.[137] Organic materials usually are inexpensive, easily processable,

and their functionality can be tailored by molecular design and chemical synthesis. On the other hand, inorganic semiconductors can also be manufactured as processable nanoparticulate colloids. By varying the size of the nano-particles, their band gap can be tuned and their absorption/emission spectra can be tailored.[138]

An effective strategy for hybrid solar cell fabrication is to use blends of nanocrystals with semiconductive polymers as bulk heterojunction.[137−142] Excitons created upon photo-excitation are separated into free charge carriers very efficiently at interfaces between organic semiconductors and inorganic semiconductor nanoparticles in a hybrid composite thin film. The solubility of the n-type and p-type components in the same solvent is an important problem. Organic semiconductors are commonly dissolved in organic solvents, whereas the inorganic semiconducting nanoparticles are commonly dissolved in aqueous solvents. Using ligand exchange, the nanoparticles can be made soluble in common organic solvents. Hybrid solar cells have been demonstrated in conjugated polymer blends containing CdSe,[139,142,143] CuInS$_2$,[137,140] CdS,[141] or PbS[144,145] nanocrystals.

The usage of inorganic semiconductor nanoparticles embedded into semiconducting polymer blends is promising for several reasons:[140]

(1) Inorganic semiconductor nanoparticles can have high absorption coefficients and higher photoconductivity as compared to many organic semiconductor materials.

(2) The n- or p-type character of the nanocrystals can be varied by synthetic routes.

(3) Band gap of inorganic nanoparticles is a function of nanoparticle size. If the inorganic nanoparticles become smaller than the size of the exciton in the bulk semiconductor (typically about 10 nm), the electronic structure of such small particles is more like those of giant molecules than an extended solid. The electronic and optical properties of such small particles depend not only on the material of which they are composed, but also on their size.[143−148] This quantum size effect can be used for novel tandem solar cells with the different band gaps by modifying only one chemical compound.

High surface tension of very small inorganic nanocrystals makes them unstable, and thus they have a tendency to grow to larger particles by a process called "Ostwald ripening".[149] Therefore, nanoparticles are synthesized commonly shielded by an organic ligand. These ligands prevent the aggregation and oxidation of the nanoparticles and can alter the solution/dispersion characteristics of the particles into the polymer matrices.[137,140]

This organic ligand, on the other hand, is a barrier for transport of charges from nanoparticle to nanoparticle. Therefore, in the hybrid solar cells, such ligands have to be removed to ensure intimate electrical contact between the nanoparticles.[145,148]

4. Conclusions and Scope

The efficiency of a solar cell is given by the open circuit voltage (V_{oc}), short circuit current density (J_{sc}), and the fill factor (FF). With a fill factor to 65% and neglecting any contribution from photons absorbed by the fullerene, Scharber et al. calculated the expected efficiency of a bulk heterojunction as a function of the band gap and the LUMO level of the donor.[63] Results shown in Figure 23[63] demonstrate that 10% solar cell efficiency is possible.

To optimize the LUMO level of the donor polymer optimizes the open circuit voltage. The charge carrier mobility of electrons and holes in the donor−acceptor blend must be as high as possible for efficient charge extraction and a high fill factor. The highest energy conversion efficiencies of around 10% are predicted by Scharber et al.[63] New novel materials have to be prepared to get to these efficiencies.[63]

Several other strategies are investigated to increase the efficiency of solar cells:[150] synthesis and development of low band gap polymers; synthesis and development of new electron-accepting materials; tandem solar cells using multiple layers of different band gaps; the use of light scattering nano- or microparticles embedded in the optically active layer to enhance the optical pathways in the film due to scattering; light trapping with simple patterning techniques;[151] hybrid
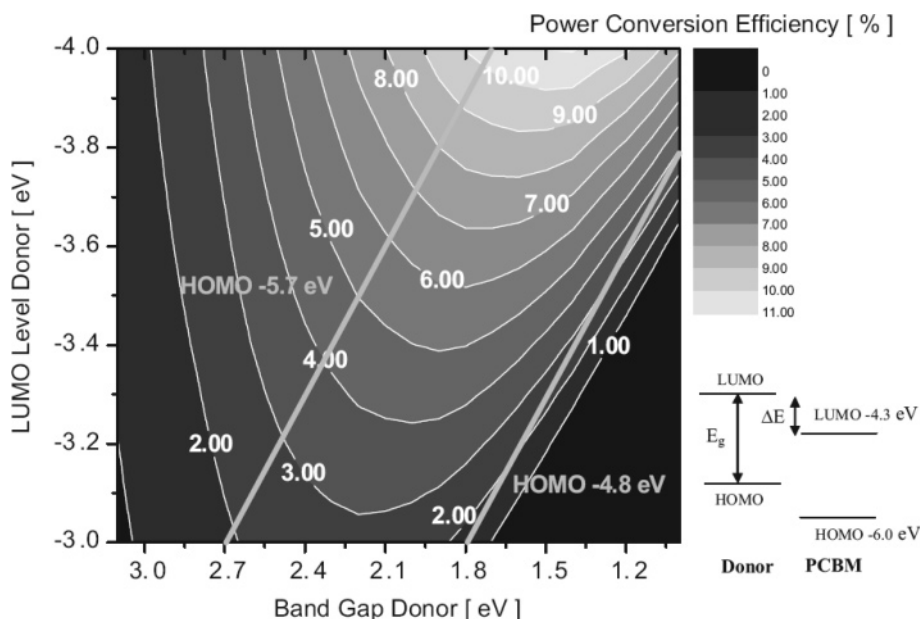
Figure 23. Contour plot showing the calculated energy-conversion efficiency (contour lines and colors) versus the band gap and the LUMO level of the donor polymer.[63] Reused with permission from M. Scharber, D. Mühlbacher, M. Koppe, P. Denk, C. Waldauf, A. Heeger, and C. Brabec, *Advanced Materials*, **18**, 789 (2006). Copyright 2006, Wiley-VCH Verlag GmbH&Co. KGaA, Weinheim.

solar cells combining the properties of inorganic semiconductor nanoparticles with conjugated polymers;[137−145] and dye sensitized solar cells (DSSCs), with organic dyes on a nanoporous TiO_2 electrode immersed in an electrolyte.[152] Recently, solar cell efficiency of 4% was reported by replacing the liquid electrolyte by an organic hole transporting medium.[153]

The ideal structure of a bulk heterojunction solar cell is schematically displayed in Figure 24. The two phases of
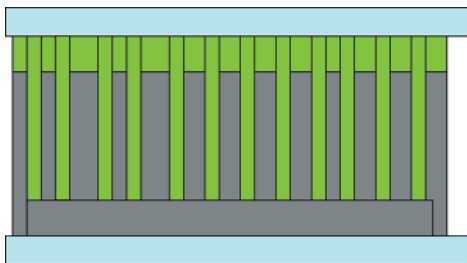
Figure 24. Ideal structure of a bulk heterojunction solar cell.

donor and acceptor within the bulk heterojunction have to be interspaced with an average length scale of around 10−20 nm equal to or less than the exciton diffusion length. The two phases have to be interdigitated in percolated highways to ensure high mobility charge carrier transport with reduced recombination. Last but not least, a pure donor phase at the hole collecting electrode and a pure acceptor phase at the electron collecting electrodes have to be placed. This minimizes the losses by recombination of the wrong sign of charges at the wrong electrode, as well as acting as diffusion barriers for the wrong sign charge carriers at the respective electrodes.

Such a well-organized nanostructure is not easy to obtain in classical polymer mixtures due to disorder. However, self-organization of the organic semiconducting polymers (molecules) can be introduced by: (1) an amphiphilic primary structure like di-block copolymers[154−156] resulting in a self-organized phase; (2) an amine-acid-type hydrogen-bonded self-organization[157] resulting in hydrogen-bonded polymeric superstructures; (3) an inorganic (ZnO_x or TiO_x) template nanostructure filled with organic semiconductors;[158,159] and (4) liquid crystalline self-organizing columns of donor−acceptor phases.[160]

Such strategies require highly interdisciplinary research between macromolecular chemistry, supramolecular chemistry, physical chemistry, colloid chemistry, photophysics/photochemistry, device physics, nanostructural analysis, and thin film technology. There are great challenges and opportunities in this avenue for the entire field of chemical sciences, and advancement is expected in interdisciplinarity.

5. Acknowledgments

6. References

(1) Tang, C. W. *Appl. Phys. Lett.* **1986**, *48*, 183.
(2) Sariciftci, N. S.; Smilowitz, L.; Heeger, A. J.; Wudl, F. *Science* **1992**, *258*, 1474.
(3) Spangaard, H.; Krebs, F. *Sol. Energy Mater. Sol. Cells* **2004**, *83*, 125.
(4) Hoppe, H.; Sariciftci, N. S.; Meissner, D. *Mol. Cryst. Liq. Cryst.* **2002**, *385*, 113.
(5) Roncali, J. *Chem. Rev.* **1997**, *97*, 173.
(6) Dimitrakopoulos, C. D.; Malenfant, P. R. L. *Adv. Mater.* **2002**, *14*, 99.
(7) Hoppe, H.; Sariciftci, N. S. *J. Mater. Chem.* **2004**, *19*, 1924.
(8) Singh, B.; Sariciftci, N. S. *Ann. Rev. Mater. Res.* **2006**, *36*, 199.
(9) *Handbook of Conductive Molecules and Polymers*; Nalwa, H. S., Ed.; John Wiley & Sons Ltd.: Chichester, 1997; Vols. 1−4.
(10) Lane, P. A.; Rostalski, J.; Giebeler, C.; Martin, S. I.; Bradley, D. D. C.; Meissner, D. *Sol. Energy Mater. Sol. Cells* **2000**, *63*, 3.
(11) Rostalski, J.; Meissner, D. *Sol. Energy Mater. Sol. Cells* **2000**, *63*, 37.
(12) Maenning, B.; Drechssel, J.; Gebeyehu, D.; Simon, P.; Kozlowski, F.; Werner, A.; Li, F.; Gundmann, S.; Sonntag, S.; Koch, M.; Leo, K.; Pfeiffer, M.; Hoppe, H.; Meissner, D.; Sariciftci, S.; Riedel, I.; Dyakonov, V.; Parisi, J. *J. Appl. Phys. A* **2004**, *79*, 1.
(13) Pfeiffer, M.; Beyer, A.; Plöninnigs, B.; Nollau, A.; Fritz, T.; Leo, K.; Schlettwein, D.; Hiller, S.; Wöhrle, D. *Sol. Energy Mater. Sol. Cells* **2000**, *63*, 83.
(14) Gebeyehu, D.; Maening, B.; Drechsel, J.; Leo, K.; Pfeiffer, M. *Sol. Energy Mater. Sol. Cells* **2003**, *79*, 81.
(15) Drechsel, J.; Mäning, B.; Kozlowski, F.; Gebeyehu, D.; Werner, A.; Koch, M.; Leo, K.; Pfeiffer, M. *Thin Solid Films* **2004**, *451−452*, 515.
(16) Allemond, P. M.; Koch, A.; Wudl, F.; Rubin, Y.; Diederich, F.; Alvarez, M. M.; Anz, S. J.; Whetten, R. L. *J. Am. Chem. Soc.* **1991**, *113*, 1050.
(17) Dresselhaus, M. S.; Dresselhaus, G.; Elklund, P. C. *Science of Fullerenes and Carbon Nanotubes.* Acedemic Press: San Diego, CA, 1996.
(18) Wudl, F. *Acc. Chem. Res.* **1992**, *25*, 157161.
(19) Shaheen, S.; Radspinner, R.; Peyghamberian, N.; Jabbour, G. *Appl. Phys. Lett.* **2001**, *79*, 2996.
(20) Hiramoto, M.; Fujiwara, H.; Yokoyama, M. *Appl. Phys. Lett.* **1991**, *58*, 1061.
(21) Geens, W.; Aernouts, T.; Poortmans, J.; Hadziioannou, G. *Thin Solid Films* **2002**, *403−404*, 438.
(22) Tsuzuki, T. T.; Shirota, J.; Rostalski, J.; Meissner, D. *Sol. Energy Mater. Sol. Cells* **2000**, *61*, 1.
(23) Rowell, M. W.; Topinka, M. A.; McGehee, M. A.; Prall, H. J.; Dennler, G.; Sariciftci, N. S.; Hu, L.; Gruner, G. *Appl. Phys. Lett.* **2006**, *88*, 233506.
(24) Frohne, H.; Shaheen, S.; Brabec, C.; Müller, D.; Sariciftci, N. S.; Meerholz, K. *ChemPhysChem* **2002**, *9*, 795.
(25) Brabec, C. J.; Shaheen, S. E.; Winder, C.; Sariciftci, N. S.; Denk, P. *Appl. Phys. Lett.* **2002**, *80*, 1288.
(26) Hung, L. S.; Tang, C. W.; Mason, N. G. *Appl. Phys. Lett.* **1997**, *70*, 152.
(27) Jabbour, G. E.; Kawahe, Y.; Shaheen, S.; Wang, J. F.; Morell, M. M.; Kippelen, B.; Peyghembarian, N. *Appl. Phys. Lett.* **1997**, *71*, 1762.
(28) Shaheen, S.; Jabbour, G.; Morrell, M.; Kawabe, Y.; Kippelen, A.; Peyghambarian, N.; Nabar, M. F.; Schlaf, R.; Mash, E. A.; Armstrong, N. R. *J. Appl. Phys.* **1998**, *84*, 2324.
(29) Jong, D.; Friedlein, M. P.; Osikowicz, R. W.; Salaneck, W. R.; Fahlman, M. *Mol. Cryst. Liq. Cryst.* **2006**, *455*, 193.
(30) Nunzi, J. M. *C. R. Physique* **2002**, *3*, 523.
(31) Miranda, P. B.; Moses, D.; Heeger, A. J. *Phys. Rev. B* **2001**, *64*, 81201.
(32) Mozer, A.; Sariciftci, S. *C. R. Chimie* **2006**, *9*, 568.
(33) Brabec, C.; Zerza, G.; Cerullo, G.; De Silvestri, S.; Luzatti, S.; Hummelen, J. C.; Sariciftci, S. *Chem. Phys. Lett.* **2001**, *340*, 232.
(34) Parker, I. *J. Appl. Phys.* **1994**, *75*, 1656.
(35) Borsenberger, P. M.; Weiss, D. S.; Borsenberger, M. B. *Organic Photoreceptors for Xerography*; Marcel Dekker Inc.: New York, 1998.
(36) Im, C.; Tian, W.; Bässler, H. A.; Fechtenkötter Watson, M. D.; Müllen, K. *J. Chem. Phys.* **2003**, *119*, 3952.
(37) Heeger, A.; Moses, D. *Primary Photoexcitations in Conjugated Polymers: Molecular Exciton versus Semiconductor Band Model*; World Scientific: Singapore, 1997.
(38) Uchida, J. X.; Rand, B. P.; Forrest, S. R. *Appl. Phys. Lett.* **2004**, *84*, 4218.
(39) Zhou, X.; Blochwitz, J.; Pfeiffer, M.; Nollau, A.; Fritz, T.; Leo, K. *Adv. Funct. Mater.* **2001**, *11*, 310.
(40) Wöhrle, D.; Meissner, D. *Adv. Mater.* **1991**, *3*, 129.
(41) Jenekhe, S. A.; Yi, S. *Appl. Phys. Lett.* **2000**, *77*, 2635.
(42) Breeze, A. J.; Salomon, A.; Ginley, D. S.; Gregg, B. A.; Tillmann, H.; Hoerhold, H. H. *Appl. Phys. Lett.* **2002**, *81*, 3085.

(43) Sariciftci, N. S.; Braun, D.; Zhang, C.; Srdanov, V. I.; Heeger, A. J.; Stucky, G.; Wudl, F. *Appl. Phys. Lett.* **1993**, *62*, 585.
(44) Halls, J. J. M.; Walsh, C. A.; Greenham, N. C.; Marseglia, E. A.; Friends, R. H.; Moratti, S. C.; Holmes, A. B. *Nature* **1995**, *78*, 451.
(45) Winder, C.; Sariciftci, N. S. *J. Mater. Chem.* **2004**, *14*, 1077.
(46) Harrison, M. G.; Gruener, J.; Spencer, G. C. W. *Phys. Rev. B* **1997**, *55*, 7831.
(47) Petterson, L. A. A.; Roman, L. S.; Inganas, O. *J. Appl. Phys.* **1999**, *86*, 487.
(48) Rotalsky, J.; Meissner, D. *Sol. Energy Mater. Sol. Cells* **2000**, *63*, 37.
(49) Hoppe, J. Ph.D. Thesis, Linz, 2004.
(50) Peumans, P.; Uchida, S.; Forrest, S. *Nature* **2003**, *425*, 158.
(51) Yu, G.; Heeger, A. J. *J. Appl. Phys.* **1998**, *78*, 4510.
(52) Yang, C. Y.; Heeger, A. J. *Synth. Met.* **1996**, *83*, 85.
(53) Halls, J. J. M.; Friend, R. *Synth. Met.* **1997**, *85*, 1307.
(54) Yu, G.; Gao, J.; Hummelen, J. C.; Wudl, F.; Heeger, A. J. *Science* **1995**, *270*, 1789.
(55) Yang, C.; Heeger, A. J. *Synth. Met.* **1996**, *83*, 85.
(56) Dittmer, J. J.; Lazzaroni, R.; Leclère, Ph.; Moretti, P. M.; Granström, Petritsch, K.; Marseglia, E. A.; Friend, R. H.; Brédas, J. L.; Rost, H.; Holmes, A. B. *Sol. Energy Mater. Sol. Cells* **2000**, *61*, 53.
(57) Dittmer, J. J.; Marseglia, E. A.; Friend, R. H. *Adv. Mater.* **2000**, *12*, 1270.
(58) Petritsch, K.; Dittmer, J. J.; Marseglia, E. A.; Friend, R. H.; Lux, A.; Rozenberg, G. G.; Moratti, S. C.; Holmes, A. B. *Sol. Energy Mater. Sol. Cells* **2000**, *61*, 63.
(59) Mende, L. S.; Fechtenkötter, A.; Müllen, K.; Moons, E.; Friend, R. H.; Mackenzie, J. D. *Science* **2001**, *293*, 1119.
(60) Padinger, F.; Rittberger, R.; Sariciftci, N. S. *Adv. Funct. Mater.* **2003**, *13*, 85.
(61) Rostalski, J.; Meissner, D. *Sol. Energy Mater. Sol. Cells* **2000**, *61*, 87.
(62) Brabec, C. J.; Cravino, A.; Meissner, D.; Sariciftci, N. S.; Fromherz, T.; Minse, M.; Sanchez, L.; Hummelen, J. C. *Adv. Funct. Mater.* **2001**, *11*, 374.
(63) Scharber, M.; Mühlbacher, D.; Koppe, M.; Denk, P.; Waldauf, C.; Heeger, A. J.; Brabec, C. *Adv. Mater.* **2006**, *18*, 789.
(64) Mallairas, G. G.; Salem, J. R.; Brock, P. J.; Scott, J. C. *J. Appl. Phys.* **1998**, *84*, 1583.
(65) Liu, L.; Shi, Y.; Yang, Y. *Adv. Funct. Mater.* **2001**, *11*, 420.
(66) Wu, C. C.; Wu, C. I.; Sturm, J. C.; Kahn, A. *Appl. Phys. Lett.* **1997**, *70*, 1348.
(67) Sugiyama, K.; Ishi, H.; Ouchi, Y.; Seki, K. *J. Appl. Phys.* **2000**, *87*, 295.
(68) Scott, J. C.; Carter, S. A.; Korg, S.; Angelopoulos, M. *Synth. Met.* **1997**, *85*, 97.
(69) Brown, J. M.; Kim, J. S.; Friend, R. H.; Caciolli, F.; Daik, R.; Feast, W. J. *Appl. Phys. Lett.* **1999**, *75*, 1679.
(70) Ganzorig, C.; Fujihira, M. *Mater. Res. Soc. Symp. Proc.* **2002**, *708*, 83.
(71) Van Duren, J. J.; Loos, J.; Morissey, F.; Leewis, C. M.; Kivits, K. P.; Vanzendoorn, L. J.; Rispens, M. T.; Hummelen, J. C.; Janssen, R. A. J. *Adv. Funct. Mater.* **2002**, *12*, 665.
(72) Bulle-Lieuwma, C. W.; VanGenip, W. J. H.; Van Duren, J. K. J.; Jankheim, P.; Janssen, R.; Niemantsverdiet, J. W. *Appl. Surf. Sci.* **2003**, *203*, 547.
(73) Van Duren, J.; Yang, X.; Loos, J.; Bulle-Lieuwma, C. W. T.; Sievel, A. B.; Hummelen, J. C.; Janssen, R. A. J. *Adv. Funct. Mater.* **2004**, *14*, 425.
(74) Hoppe, H.; Glatzel, T.; Niggemann, M.; Schwinger, W.; Schaeffler, F.; Hinsch, A.; Lux-Steiner, M.; Sariciftci, N. S. *Thin Solid Films* **2006**, *511-512*, 587.
(75) Hoppe, H.; Niggemann, M.; Winder, C.; Kraut, J.; Hiesgh, R.; Hinsch, A.; Meissner, D.; Sariciftci, N. S. *Adv. Funct. Mater.* **2004**, *14*, 1005.
(76) Gebeyehu, D.; Brabec, C. J.; Padinger, F.; Fromherz, T.; Hummelen, J. C.; Badt, D.; Schindler, H.; Sariciftci, N. S. *Synth. Met.* **2001**, *118*, 1.
(77) Martens, T.; Hoen, J. D.; Munters, T.; Beelen, Z.; Goris, L.; Monca, J.; Oliesloeger, M. D.; Vanderzende, D.; De Schopper, L.; Andriessen, R. *Synth. Met.* **2003**, *138*, 243.
(78) Arias, A. C.; MacKenzie, J. D.; Stevenson, R.; Halls, J. M.; Inbasekaran, M.; Woo, E. P.; Richards, D.; Friend, R. H. *Macromolecules* **2001**, *34*, 6005.
(79) Gadisa, A.; Svensson, M.; Andersson, M. R.; Inganäs, O. *Appl. Phys. Lett.* **2004**, *84*, 1609.
(80) Riedel, I.; Dyakonov, V. *Phys. Status Solidi A* **2004**, *201*, 1332.
(81) Kroon, J. M.; Veenstra, S. C.; Sloof, L. H.; Verhees, W. J. H.; Koetse, M. M.; Sweelssen, J.; Schoo, H. F. M.; Beek, W. J. E; Wienk, M. M.; Janssen, R. A. J.; Yang, X.; Loos, J.; Mihailetchi, V. D.; Blom, P. W. M.; Knol, J.; Hummelen, J. C. *Abst. Eur. Sol. Energy Conf.* **2005**.
(82) Neugebauer, H. *Electrochem. Soc., Proc.* **2002**, *12*, 19.
(83) Liedenbaum, A. J. F.; Vleggaar, J. J. M., *Philips Journal of Research*, **1998**, *51*, 511.
(84) Schuler, S. *Appl. Phys. A* **2003**, *79*, 37.
(85) Yang, X.; Van Duren, J. K. J.; Janssen, R. A. J.; Michels, M. A. J.; Loos, J. *Macromolecules* **2004**, *37*, 2151.
(86) Drees, M.; Hoppe, H.; Winder, C.; Neugebauer, H.; Sariciftci, N. S.; Schwinger, W.; Schäffler, F.; Topf, C.; Scharber, C.; Gaudiana, R. *J. Mater. Chem.* **2005**, *15*, 5158.
(87) Yang, X.; Loos, J.; Veenstra, S. C.; Verhees, W. J. H.; Wienk, M.; Kroon, M.; Michels, M. H. J.; Janssen, R. A. J *Nano Lett.* **2005**, *5*, 579.
(88) Shaheen, S.; Brabec, C. J.; Sariciftci, N. S.; Padinger, F.; Fromherz, T.; Hummelen, J. C. *Appl. Phys. Lett.* **2001**, *78*, 841.
(89) Wienk, M.; Kroon, J. M.; Verhees, W. J. H.; Hummelen, J. C.; Van Hal, P. A.; Janssen, J. *Angew. Chem., Int. Ed.* **2003**, *42*, 3371.
(90) Yokoyama, H.; Kramer, E. J.; Rafailovich, M. H.; Sokolov, J.; Schwarz, S. A. *Macromolecules* **1998**, *31*, 8826.
(91) Mozer, A. J.; Dennler, G.; Sariciftci, N. S.; Westerling, M.; Pivrikas, A.; Österbacka, R.; Juska, G. *Phys. Rev. B* **2005**, *72*, 35217.
(92) Pivrikas, A.; Juska, G.; Mozer, A. J.; Scharber, M.; Karlauskas, A.; Sariciftci, N. S.; Stubb, H.; Österbacka, R. *Phys. Rev. Lett.* **2005**, *94*, 176806.
(93) Mozer, A. J.; Sariciftci, N. S.; Lutsen, L.; Vanderzande, D.; Österbacka, R.; Westerling, M.; Juska, G. *Appl. Phys. Lett.* **2005**, *86*, 112104.
(94) Mozer, A. J.; Sariciftci, N. S.; Pivrikas, A.; Österbacka, R.; Juska, G.; Brassat, L. H. *Phys. Rev. B* **2005**, *71*, 35214.
(95) Mozer, A.; Sariciftci, N. S. *Chem. Phys. Lett.* **2004**, *389*, 438.
(96) Mozer, A. Ph.D. Thesis, Linz, 2004.
(97) Pacios, R.; Bradley, D. D.; Nelson, J.; Brabec, C. J. *Synth. Met.* **2003**, *137*, 1469.
(98) Mihailetchi, V.; Van Duren, K. K.; Blom, P.; Hummelen, J. C.; Janssen, R.; Kroon, J.; Rispens, M.; Verhees, W.; Wienk, M. *Adv. Funct. Mater.* **2006**, *16*, 699.
(99) Arbogast, J. W.; Foote, C. S. *J. Am. Chem. Soc.* **1991**, *113*, 886.
(100) Wienk, M.; Kroon, J. M.; Verhees, W. J. H.; Krol, J.; Hummelen, J. C.; Van Haal, P.; Janssen, R. A. J. *Angew. Chem., Int. Ed.* **2003**, *42*, 3371.
(101) Chirvaze, D.; Chiguvare, Z.; Knipper, M.; Parisi, J.; Dyakonov, V.; Hummelen, J. C. *J. Appl. Phys.* **2003**, *93*, 3376.
(102) Chirvaze, D.; Parisi, J.; Hummelen, J. C.; Dyakonov, V. *Nanotechnology* **2004**, *15*, 1314.
(103) Reyes, R. R.; Kim, K.; Carroll, D. L. *Appl. Phys. Lett.* **2005**, *87*, 083506.
(104) Al Ibrahim, M.; Klaus Roth, H.; Schroedner, M.; Kalvin, A.; Zhokhavets, U.; Gobsch, G.; Scharff, P.; Sensfuss, S. *Org. Electron.* **2005**, *6*, 65.
(105) Ahn, T.; Choi, B.; Ahn, S. N.; Han, S. N.; Lee, H. *Synth. Met.* **2001**, *117*, 219.
(106) Chirvaze, D.; Chiguvare, Z.; Knipper, M.; Parisi, J.; Dyakonov, V.; Hummelen, J. C. *Synth. Met.* **2003**, *138*, 299.
(107) Takahashi, K.; Tsuji, K.; Inote, K.; Yamaguchi, T.; Kanura, T.; Murata, K. *Synth. Met.* **2004**, *130*, 177.
(108) Schilinsky, P.; Waldauf, P.; Brabec, C. J. *J. Appl. Phys. Lett.* **2002**, *81*, 3885.
(109) Kim, J.; Kim, S.; Lee, H.; Lee, K.; Ma, W.; Huong, X.; Heeger, A. J. *Adv. Mater.* **2006**, *18*, 572.
(110) Prosa, T. J.; Winokur, M. J.; Moulton, M. M.; Smith, P.; Heeger, A. J. *Macromolecules* **1992**, *25*, 4364.
(111) Bao, Z.; Dodabalapur, A.; Lovinger, A. *Appl. Phys. Lett.* **1996**, *69*, 4108.
(112) Sirringhaus, H.; Tessler, N.; Friend, R. H. *Science* **1998**, *280*, 1741.
(113) Mihailetchi, V. D.; Van Duren, J. K. J.; Blom, P. W. M.; Hummelen, J. C.; Janssen, R. A. J.; Kroon, J. M.; Rispens, M. T.; Verhees, W. J. H.; Wienk, M. M. *Adv. Funct. Mater.* **2003**, *13*, 43.
(114) Camaioni, N.; Ridolfi, G.; Casalbore, G. M.; Possamai, G.; Maggini, M. *Adv. Mater.* **2002**, *14*, 1735.
(115) Ahn, T.; Sein Holta, H. L. *Appl. Phys. Lett.* **2002**, *80*, 392.
(116) Brown, P. J.; Thomas, D. S.; Köhler, A.; Wilson, J.; Kim, J. S.; Rainsdale, C.; Sirringhaus, H.; Friend, R. H. *Phys. Rev. B* **2003**, *67*, 064203.
(117) Zhang, F.; Svensson, M.; Andersson, M.; Maggini, M.; Bucella, S.; Menna, E.; Inganäs, O. *Adv. Mater.* **2001**, *13*, 1871.
(118) Al Ibrahim, M.; Ambacher, O.; Sensfuss, S.; Gobsch, G. *Appl. Phys. Lett.* **2005**, *86*, 201120.
(119) Al Ibrahim, M.; Roth, H. K.; Zhokhavets, U.; Gobsch, G.; Sensfuss, S. *Sol. Energy Mater. Sol. Cells* **2005**, *85*, 13.
(120) Theander, M.; Inganäs, O.; Mamo, W.; Olinga, T.; Svensson, M.; Andersson, M. *J. Phys. Chem. B* **1999**, *103*, 7771.
(121) Erb, T.; Zhokhavets, U.; Gobsch, G.; Raleva, S.; Stühn, B.; Schilinsky, P.; Waldauf, C.; Brabec, C. J. *Adv. Funct. Mater.* **2005**, *15*, 1193.
(122) Zhochhavets, U.; Erb, T.; Gobsch, G.; Al Ibrahim, M.; Ambacher, O. *Chem. Phys. Lett.* **2006**, *418*, 347.

(123) Savenije, T. J.; Kroeze, J. E.; Yang, X.; Loos, J. *Adv. Funct. Mater.* **2005**, *15*, 1260.

(124) Sirringhaus, H.; Brown, P. J.; Friend, R. H.; Nielsen, N. M.; Bechgerard, K.; Langeveld, B. M. W.; Spiening, A. J. H.; Janssen, R. A. J.; Meijer, E. W.; Herwig, P.; De Leeuw, D. M. *Nature* **1999**, *401*, 685.

(125) Kline, R. J.; Mcgehee, M. D.; Kadnikova, E. N.; Liu, J. S.; Frechet, J. M. J. *Adv. Mater.* **2003**, *15*, 1519.

(126) Kim, Y.; Cook, S.; Choulis, S. A.; Nelson, J.; Durrant, J.; Bradley, D. *Chem. Mater.* **2004**, *16*, 4812.

(127) Goh, C.; Kline, R. J.; McGehee, M. D.; Kadnikova, E. N.; Liu, J. S.; Frechet, J. M. J. *Appl. Phys. Lett.* **2005**, *86*, 122110.

(128) Mihailetci, V. D.; Xie, H.; Boer, B.; Koster, L. A.; Blom, P. W. M. *Adv. Funct. Mater.* **2003**, *13*, 49.

(129) Mihailetci, V. D.; Koster, L. J. A.; Blom, P. W. M.; Melzer, C.; Boer, B.; Van Duren, J. K. J.; Janssen, R. A. J. *Adv. Funct. Mater.* **2005**, *15*, 795.

(130) Koster, L. J. A.; Smits, E. C. P.; Mihailetci, V. D.; Blom, P. W. M. *Phys. Rev. B* **2005**, *72*, 085205.

(131) Mihailetchi, V. D.; Koster, L. J. A.; Hummelen, J. C.; Blom, P. W. M. *Phys. Rev. Lett.* **2004**, *93*, 216601.

(132) Melzer, C.; Koop, E. J.; Mihailetchi, V. D.; Blom, P. W. M. *Adv. Funct. Mater.* **2004**, *14*, 865.

(133) Hoppe, H.; Sariciftci, N. S. *Thin Solid Films* **2004**, *451−452*, 589.

(134) Kroon, J. M.; Veenstra, S. C.; Sloof, L. H.; Verhees, W. J. H.; Koetse, M. M.; Sweelssen, J.; Schoo, H. F. M.; Beek, W. J. E; Wienk, M. M.; Janssen, R. A. J.; Yang, X.; Loos, J.; Mihailetchi, V. D.; Blom, P. W. M.; Knol, J.; Hummelen, J. C. *Abst. Eur. Sol. Energy Conf.* **2005**.

(135) Cravino, A.; Sariciftci, N. S. *J. Mater. Chem.* **2002**, *12*, 1931.

(136) Cravino, A.; Sariciftci, N. S. *Nat. Mater.* **2003**, *2*, 360.

(137) Arici, E.; Sariciftci, N. S.; Meissner, D. *Adv. Funct. Mater.* **2003**, *2*, 13.

(138) Weller, H. *Angew. Chem., Int. Ed. Engl.* **1993**, *32*, 41.

(139) Hunyh, W.; Dittmer, J.; Alivisatos, A. P. *Science* **2002**, *295*, 2425.

(140) Arici, E.; Meissner, D.; Schäffler, F.; Sariciftci, N. S. *Int. J. Photoenergy* **2003**, *5*, 199.

(141) Greenham, N. C.; Peng, X.; Alivisatos, A. P. *Phys. Rev. B* **1996**, *54*, 17628.

(142) Huynh, W.; Peng X.; Alivisatos, A. P. *Adv. Mater.* **1999**, *11*, 11.

(143) Alivisatos, A. P. *Science* **1996**, *271*, 933.

(144) McDonald, S.; Konstantanos, G.; Zhang, S.; Cyr, P. W.; Levira, L.; Sargent, H. *Nat. Mater.* **2005**, *4*, 138.

(145) Günes, S.; Fritz, K.; Neugebauer, H.; Sariciftci, N. S.; Kumar, S.; Scholes, G. *Sol. Energy Mater. Sol. Cells* **2006**, *91*, 420.

(146) Steigerwald, M. L.; Eisrus, L. *Acc. Chem. Res.* **1990**, *23*, 283.

(147) Murphy, C. J.; Coffer, J. L. *Appl. Spectrosc.* **2002**, *56*, 16.

(148) Empedocles, S. A.; Bavendi, M. G. *Acc. Chem. Res.* **1999**, *32*, 389.

(149) Black, C. T.; Murray, C. B.; Sandstrom, R. L.; Sun, S. *Science* **2000**, *290*, 1131.

(150) Brabec, C.; Winder, C.; Sariciftci, N. S.; Hummelen, J. C.; Dhanabalan, A.; van Hal, P. A.; Janssen, R. A. *Adv. Funct. Mater.* **2002**, *12*, 709.

(151) Roman, L. S.; Inganäs, O.; Granlund, T.; Nyberg, T.; Svensson, M.; Andersson, M. R.; Hummelen, J. C. *Adv. Mater.* **2000**, *12*, 189.

(152) O'Reagan, B.; Graetzel, M. *Nature* **1991**, *353*, 737.

(153) Mende, L. S.; Graetzel, M. *Thin Solid Films* **2006**, *500*, 296.

(154) Jenekhe, S.; Chen, X. L. *Science* **1998**, *279*, 1903.

(155) *Semiconducting Polymers*; Hadziioannou, G., von Hutten, F., Eds.; Wiley−VCH: Weinheim, 2000.

(156) *Organic Photovoltaics*; Sariciftci, N. S., Sun, S. S., Eds.; Taylor & Francis: London, 2005.

(157) Rispens, M. T.; Sanchez, L.; Beckers, E. H. A.; van Hal, P. A.; Schenning, A.; El-ghayoury, Peeters, E.; Meijer, B.; Janssen, R.; Hummelen, J. C. *Synth. Met.* **2003**, *135*, 801.

(158) Olsa, D. C.; Piris, J.; Collins, R. T.; Shaheen, S.; Ginley, D. *Thin Solid Films* **2006**, *496*, 26.

(159) Coakley, K.; McGehee, M. D. *Appl. Phys. Lett.* **2003**, *83*, 3380.

(160) Tracz, A.; Jeszka, J. K.; Watson, M. D.; Pisula, W.; Mullen, K.; Pakula, T. *J. Am. Chem. Soc.* **2003**, *125*, 1682.